

- HUGHES, E. W. (1941). *J. Amer. Chem. Soc.* **63**, 1737.  
*International Tables for X-ray Crystallography* (1962). Vol. III. Birmingham: Kynoch Press.
- JELLINEK, F. (1958). *Acta Cryst.* **11**, 677.
- JELLINEK, F. (1959). *Z. Naturforsch.* **14b**, 737.
- JONES, N., MARSH, R. E. & RICHARDS, J. H. *Acta Cryst.* **19**, 330.
- KEIDEL, F. A. & BAUER, S. H. (1956). *J. Chem. Phys.* **25**, 1218.
- MCWEENY, R. (1954). *Acta Cryst.* **7**, 180.
- RINEHART, K. L., JR., FRERICHS, A. K., KITTLE, P. A., WESTMAN, K. F., GUSTAFSON, D. H., PRUETT, R. L. & MCMAHON, J. E. (1960). *J. Amer. Chem. Soc.* **82**, 4111.
- ROBERTSON, J. M. (1953). *Organic Crystals and Molecules*, p. 213. Ithaca: Cornell Univ. Press.
- ROLLETT, J. S. & SPARKS, R. A. (1960). *Acta Cryst.* **13**, 273.
- SEIBOLD, E. A. & SUTTON, L. E. (1955). *J. Chem. Phys.* **23**, 1967.
- STRUCHKOV, Y. T. & KHOTSYANOVA, T. L. (1957). *Kristallografia*, **2**, 382.

*Acta Cryst.* (1965). **19**, 381

## The Crystal Structure of the Serpentine Mineral, Lizardite $\text{Mg}_3\text{Si}_2\text{O}_5(\text{OH})_4$

By J. C. RUCKLIDGE AND J. ZUSSMAN

*Department of Geology and Mineralogy, University of Oxford\*, England*

(Received 8 December 1964)

Lizardite from Kennack Cove, Cornwall, England, is an unusual serpentine in being sufficiently coarse-grained for single-crystal X-ray analysis. The basic layered serpentine structure is confirmed for this specimen but the crystals are found to be disordered in three different ways. (1) The crystals are macroscopically bent about more than one axis. (2) Some of the layers are displaced by  $\pm b/3$ . (3) Some of the layers are rotated by  $180^\circ$ . The broadened reflexions resulting from each of these factors have been examined and, within the limits imposed by them, the structural detail has been refined. The inter-layer repeat is  $c=7.3 \text{ \AA}$  and individual layers have trigonal symmetry with  $a=5.3 \text{ \AA}$ .

Two types of serpentine mineral have been well characterized, chrysotile by its fibrous habit with fibre repeat distance  $5.3 \text{ \AA}$ , and antigorite with its super-period in the  $a$  direction. Much massive serpentine has neither of these features and has been termed lizardite (Whittaker & Zussman, 1956). Electron microscopic examination of lizardite shows essentially platy particles in which the intra-layer orthogonal repeat distances are simply  $a=5.3$ ,  $b=9.2 \text{ \AA}$ , and the X-ray powder patterns in general show no evidence of other than a single-layered cell with  $c \simeq 7.3 \text{ \AA}$  and  $\beta=90^\circ$ . The detailed structure of individual serpentine layers (Fig. 1) has been assumed, by virtue of the chemical formula,  $\text{Mg}_3\text{Si}_2\text{O}_5(\text{OH})_4$ , and cell parameters, to be a trioctahedral analogue of the single kaolinite layer; complex distorted versions of this have been shown to comprise the structures of chrysotile (Whittaker, 1956a) and antigorite (Kunze, 1956, 1958, 1961), but no direct evidence of the simple structure has hitherto been presented for lizardite, because of the difficulty of obtaining single crystals large enough for X-ray diffraction work. One specimen of lizardite, however, offers the possibility of single-crystal X-ray work, namely that from Kennack Cove, Cornwall (Midgley, 1951; Whittaker & Zussman, 1956), since its crystallite size, though small, is manageable from this point of view. It has

emerged after study of this specimen that the extent to which the structure can be determined in detail is limited even in this case because of the existence of different kinds of imperfections, the most obvious of which is that the crystals are considerably bent.

### Experimental

#### *X-ray powder pattern*

The powder pattern given in Table 1 is more complete than that given by Whittaker & Zussman (1956) and is indexed with an ortho-hexagonal unit cell having  $a=5.31$ ,  $b=9.2$  ( $\simeq \sqrt{3}a$ ),  $c=7.31 \text{ \AA}$ ,  $\beta=90^\circ$ .

Table 1. *Lizardite powder pattern*

Cu  $K\alpha$  radiation, 11.46 cm diameter camera  
 Indices on basis of cell with  $a=5.31$ ,  $b=9.20$ ,  $c=7.31 \text{ \AA}$ ,  $\beta=90^\circ$

$d_{\text{obs.}}$	$d_{\text{calc.}}$	$hkl$	$I$
7.4 $\text{\AA}$	7.31 $\text{\AA}$	001	<i>vs</i>
4.6	4.60	020	<i>s</i>
3.9	3.89	021	<i>m</i>
3.67	3.66	002	<i>s</i>
2.875	2.862	022	<i>vw</i>
2.663	2.655	200	<i>mw</i>
2.505	2.496	201	<i>vs</i>
2.410	2.437	003	<i>vvw</i>
2.307	2.300	040	<i>vvw</i>
2.156	2.148	202	<i>s</i>
1.945	1.947	042	<i>vvw</i>
1.835	1.828	004	<i>vw</i>
1.799	1.795	203	<i>m</i>
1.743	1.738	310	<i>mw</i>

\* This work was begun while the authors were at the Department of Geology, University of Manchester.

Table 1 (cont.)

$d_{obs.}$	$d_{calc.}$	$hkl$	$I$
1.692	1.691	311	$vw$
1.572	1.570	312	$vw$
1.538	1.533	060	$s$
1.505	1.503	061, 204	$s$
1.462	1.462	005	$vw$
1.416	1.414	062	$m$
1.332	1.328	400	$w$
1.310	1.306	401	$ms$
1.281	1.281	205	$m$
1.253	1.248	402	$w$
1.219	1.218	006	$vw$
1.169	1.166	403	$m$
1.110	1.107	206	$vw$
1.078	1.074	404	$w$
1.058	1.055	510, 065	$w$
1.045	1.044	007	$vw$
1.002	1.004	530	$vw$
0.993	0.994	531	$m$
0.981	0.983	405	$vw$
0.968	0.968	532	$w$
0.952	0.954	066	$w$
0.923	0.928	533	$w$
0.912	0.914	008	$vw$
0.885	0.885	600	$m$
0.880	0.879	601, 504	$vw$
0.861	0.862	067,208,602	$m$
0.834	0.832	603	$vw$
0.828	0.821	407	$vw$
0.786	0.785	068	$vw$

Oscillation photographs

All crystals are visibly bent but the smallest crystals and those with least curvature were selected for study by single-crystal X-ray methods. Oscillation photographs about the  $x$  and  $y$  axes gave reflexions most of which were streaked along Debye arcs. For reflexions

$hkl$  including  $h0l$ ,  $0kl$  and  $00l$ , the length of arc increased with  $l$  and  $h00$ ,  $0k0$  and  $hk0$  were all relatively unstreaked in this respect. Although the latter reflexions were sharp compared with others on the film, they were nevertheless somewhat broader than those from the average well-crystallized material. Attempts to index reflexions by means of a  $15^\circ$  lune and the reciprocal lattice, showed that reflexions outside the lune were being recorded on the film.

Because of the crystal habit (platy perpendicular to  $c$ ),  $z$  axis oscillation photographs were unsatisfactory, but it could be seen that on these,  $0k0$  and  $h00$  reflexions were streaked.

In addition to the above features, the  $x$  and  $y$  axis photographs showed that reflexions  $hkl$  with  $k \neq 3m$  ( $m = \text{integer or zero}$ ) were spread laterally along layer lines as well as along powder arcs. The combination of the two types of spot extension leads in certain cases (e.g.  $020, 110$ ) to the appearance of small fan-shaped regions of blackening on the film, as illustrated in Fig. 2, an oscillation photograph about the  $x$  axis.\*

Reflections with  $(h+k)$  odd are absent, indicating that the lattice is  $C$  face centred.

Stationary crystal photographs

Photographs were taken with the crystal in a succession of azimuthal settings about the  $x$  and  $y$  axes, thus exploring the distribution of reflexions in reciprocal space.

\* A weak fan-shaped region is shown also near the reflexion 130; this is caused by an intermediate diffuse reflexion between 130 and 131 (see p. 383).

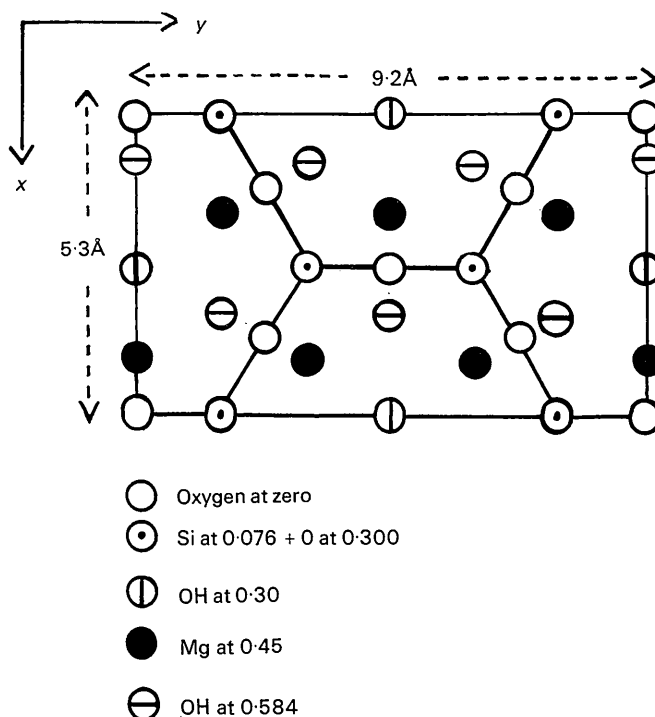


Fig. 1.  $z$ -axis projection of a single-layer unit cell of lizardite.

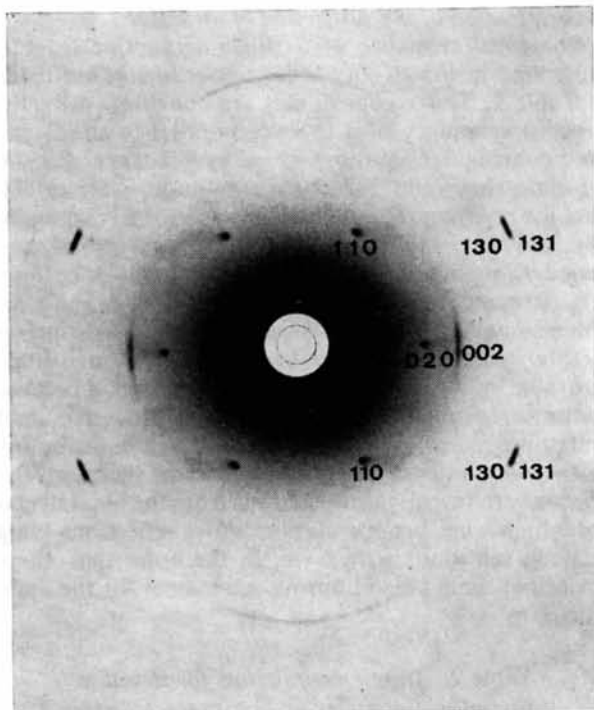


Fig. 2. Central portion of an  $x$ -axis rotation photograph of lizardite, showing arc and fan shaped spreading of certain reflexions.

#### Weissenberg photographs

Zero and first layer equi-inclination photographs were taken about the  $x$  axis, and zero and third layer photographs about  $y$ . All reflexions were elongated parallel to the camera axis (lines of constant  $2\theta$ ) corresponding to their extension into Debye arcs on rotation and oscillation photographs. Reflexions for which  $k \neq 3m$  were in addition extended in the direction of  $c^*$  along the curves of the Weissenberg festoons of constant  $h$  and  $k$ .

A most interesting feature of the Weissenberg photographs was the presence of weak very diffuse maxima lying between successive integral reflexions along the Weissenberg festoons of constant  $h$  and  $k$ . These re-

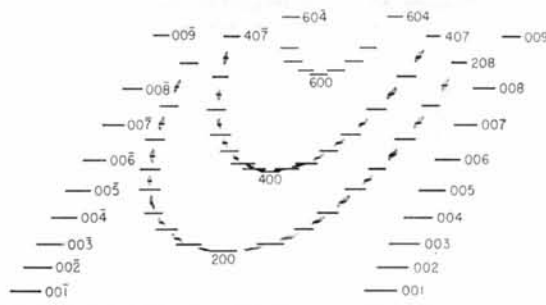


Fig. 3. Diagram illustrating  $y$ -axis zero layer Weissenberg photograph. All reflexions are streaked parallel to the camera axis; intermediate reflexions occur along  $20l$  and  $40l$  festoons but not along  $60l$ .

flexions with  $l \approx (m + \frac{1}{2})$  occur where  $k = 3m$  (for  $k \neq 3m$  the main reflexions are themselves extended), but not where  $h$  is also a multiple of 3. Thus the Weissenberg rows  $20l$ ,  $40l$  have the intermediate maxima but  $60l$  does not,  $13l$  does but  $33l$  does not,  $26l$  does but  $06l$  does not. The diffuse reflexions are of rather weak intensity and are not easily shown on a photographic print: a typical Weissenberg photo ( $y$ -axis zero layer) is shown diagrammatically therefore in Fig. 3.

Weissenberg photographs of over a dozen different crystals were taken and the nature of the intermediate maxima was found to vary from one crystal to another. In some, the intermediate maxima were extremely diffuse as shown in Fig. 3, in some they were as sharp as the main reflexions though very much weaker, while in others moderate diffuseness was shown. One crystal showing sharp intermediate reflexions at  $l \approx m + \frac{1}{2}$  also showed very weak diffuse reflexions at  $l \approx m \pm \frac{1}{4}$ .

In the initial stages of the structure determination the extra weak reflexions were ignored. Variation between crystals was not appreciated at this time and so only one crystal, of the type giving diffuse intermediate reflexions at  $l \approx m + \frac{1}{2}$ , was used for intensity measurements.

An intensity scale was prepared using a suitable 'powder streak' from a Weissenberg photograph using a small oscillation angle and a crystal similar to that used to record all other intensities. The intensities of all reflexions, except those expanded in the  $c^*$  direction, were measured by visual comparison, corrected for Lorentz and polarization effects, and converted to amplitudes in the usual way. No crystal shape or absorption correction appeared to be necessary. The values of these amplitudes after scaling to  $F_c$ 's for an approximately correct structure are listed under  $F_o$  in Table 3.  $00l$  reflexions were measured on  $x$  and  $y$  zero-layer photographs,  $20l$ ,  $40l$ ,  $60l$  on  $y$  zero layer,  $06l$  on the  $x$  axis zero layer,  $53l$  and  $19l$  on the third  $y$  and first  $x$  layer respectively.

The profiles of the intermediate diffuse reflexions were measured with a microdensitometer. For several of these peaks the integral breadth  $b$ , defined as the width of the rectangle with the same height and the same area as that under the peak, varied between 0.3 and 0.4, with an average of 0.35 (units of  $c^*$ ).

#### Precession photographs

A precession camera was used in order to examine the profiles of the reflexions  $hkl$  with  $k \neq 3m$ , and the integral breadths of six peaks measured ranged between 0.38 and 0.55, with a mean of 0.47.

#### Interpretation

##### Symmetry

Measurement of intensities on Weissenberg photographs showed that the crystal structure has trigonal symmetry, or approximates closely to it, since the following intensities were equal within the limits of ex-

perimental error (indexing is for the ortho-hexagonal cell):

$$\begin{array}{ll} 20l = 13\bar{l} = \bar{1}3l & 20\bar{l} = 13l = \bar{1}3\bar{l} \\ 40l = 26\bar{l} = \bar{2}6l & 40\bar{l} = 26l = \bar{2}6\bar{l} \\ 0\bar{5}l = 33l & 53\bar{l} = 19l = \bar{1}9\bar{l} \\ 53l = 19\bar{l} = \bar{5}3l & \end{array}$$

The intensities also showed the presence of a mirror plane perpendicular to  $y$ . Thus for lizardite the unit cell is not only dimensionally trigonal, but the structure is trigonal too. The indexing on the basis of the ortho-hexagonal cell was maintained nevertheless, for convenience of computation and for ease of comparison with other serpentine minerals.

A further feature noted was, that whereas the intensities of pairs of reflexions  $hkl$  and  $hk\bar{l}$  were in general unequal, they were equal if  $h$  and  $k$  were both multiples of three.

#### Powder arcs and crystal bending

In oscillation or rotation photographs about the  $x$  axis, bending of the crystal about the  $x$  axis will not cause spreading of the reflexions recorded on the cylindrical film. Bending of the crystal about the  $y$  axis will cause spreading along powder arcs and the spread will be absent for  $0k0$  reflexions, small for  $hk0$  reflexions and greatest for  $0kl$  reflexions. For the latter and for  $hkl$  reflexions the spread will increase with increasing value of  $l$ . The observed reflexions follow approximately this scheme, indicating a degree of crystal bending about  $y$ , and moreover in the  $y$ -axis oscillation and rotation photographs the spreading of various reflexions is consistent with bending of the crystal about  $x$ . The observed effects are somewhat more complex because bending about the two axes is occurring simultaneously, and it is inferred from all types of photograph taken that the crystal shape is approximately that of a spherical cap.

Further evidence of crystal bending was provided by the series of stationary crystal photographs exploring reciprocal space, and also by the extension of spots on Weissenberg photographs parallel to the camera axis.

From measurements made on the various kinds of photograph it was estimated that the angle of bending was approximately  $12^\circ$  for a crystal of average diameter about 0.3 mm.

The above description relates only to the reflexions with  $k=0$  or  $3m$ ; for those with  $k \neq 3m$  additional features are superimposed upon the powder arcs. When  $k \neq 3m$  streaks parallel to  $c^*$  occur in reciprocal space instead of spots, and when the various bending operations are applied to these the result is a 'wheat sheaf' distribution which, when cut by the reflecting sphere, produces a fan-shaped area of blackening on a rotation photograph. This is illustrated in Fig. 2, and from the spread of the fan it can be shown that the reciprocal lattice rods are tilted through about  $12^\circ$ .

#### Determination of $h0l$ projection of structure

The ideal structure of a single serpentine layer is illustrated in Fig. 1, and atomic coordinates are listed in Table 2. The  $x$  coordinates are consistent with the trigonal symmetry of a layer ( $c$  parallel to triad) and the  $z$  coordinates are those found by Whittaker (1956a) for clino-chrysotile. Structure amplitudes were calculated for a structure with these sheets stacked orthogonally, and the comparison of  $F_o$ 's (from one crystal) and scaled  $F_c$ 's gave an  $R$  index of 26% [Table 3, column (c)]. Attempts to refine this structure by one- and two-dimensional Fourier syntheses and by least-squares methods yielded no improvement in  $R$ . Although some errors in intensity estimation no doubt occur because of the spreading of Weissenberg spots, it was thought that some factor other than this was also contributing to the poor intensity agreement. It was therefore felt necessary to investigate deviations from the ideal structure which were producing the diffuse reflections lying between reflexions with  $l=m$ , in the hope that these deviations would also improve agreement for the main reflexions.

Table 2. Atomic coordinates for lizardite  
Coordinates of atoms ( $x, y, z$ ), ( $\frac{1}{2} + x, \frac{1}{2} + y, z$ )

	$x$	$y$	$z^*$
O	0	0	0
O	0.250	0.250	0
O	0.750	0.250	0
Si	0	0.167	0.076
Si	0.500	0.333	0.076
O	0	0.167	0.300
O	0.500	0.333	0.300
OH	0.500	0	0.300
Mg	0.333	0.167	0.450
Mg	0.333	0.500	0.450
Mg	0.333	0.833	0.450
OH	0.167	0	0.584
OH	0.167	0.333	0.584
OH	0.167	0.667	0.584

\*  $z$  coordinates given in fractions of a one layer repeat.

Table 3. Comparison of  $F_o$  and  $F_c$  for lizardite (a) using structure model 2 (see text), (b) using structure model 3, (c) for regular one-layer structure

Sets of reflexions which are related to those below by trigonal symmetry are not listed

$hkl$	$F_o$	$F_c(a)$	$F_c(b)$	$F_c(c)$
001	22	32	32	32
02	34	48	48	48
03	17	22	22	22
04	23	22	22	22
05	26	27	27	27
06	25	28	28	28
07	19	25	25	25
08	21	28	28	28
09	5	12	12	12
200	17	11	11	11
01	49	42	43	52
02	35	31	36	46
03	32	29	35	47
04	27	31	36	37
05	21	20	25	12

Table 3 (cont.)

<i>hkl</i>	<i>F<sub>o</sub></i>	<i>F<sub>c</sub>(a)</i>	<i>F<sub>c</sub>(b)</i>	<i>F<sub>c</sub>(c)</i>
06	17	12	15	21
07	14	15	16	12
08	12	11	12	14
01̄	35	29	31	19
02̄	24	16	24	18
03̄	18	6	21	14
04̄	31	35	40	46
05̄	30	36	38	48
06̄	11	6	11	10
07̄	17	19	20	23
08̄	10	8	9	8
400	28	21	21	21
01	37	32	33	25
02	22	13	18	24
03	20	15	21	4
04	30	30	33	40
05	23	18	21	28
06	8	8	11	14
07	7	9	10	13
01̄	40	41	42	49
02̄	15	8	15	16
03̄	33	32	35	44
04̄	20	21	25	21
05̄	11	7	13	9
06̄	8	3	8	9
07̄	7	7	8	8
600	35	35	35	35
01	19	17	17	17
02	14	13	13	13
03	13	11	11	11
04	7	9	9	9
01̄	19	17	17	17
02̄	14	13	13	13
03̄	13	11	11	11
04̄	7	9	9	9
060	62	57	57	57
1	33	29	29	29
2	24	19	19	19
3	20	16	16	16
4	14	12	12	12
5	23	25	25	25
6	22	28	28	28
7	12	15	15	15
8	17	30	30	30
530	17	9	9	9
1	40	24	25	30
2	20	14	17	21
3	23	17	20	27
4	22	20	23	24
5	11	14	16	9
1̄	27	17	18	11
2̄	20	11	14	15
3̄	9	3	12	7
4̄	28	22	25	29
5̄	24	23	25	31

R = 20.8 R = 18.0 R = 25.8

*Diffraction maxima at non-Bragg angles*

Since, for the crystal first studied, the additional diffuse maxima occur approximately half way between main reflections along reciprocal lattice rows parallel to *c*<sup>\*</sup>, a first approximation to their interpretation is to regard them as evidence that some component of the structure has a two-layered unit cell. The relationship between oxygen atoms at the bases of tetrahedra of one layer and hydroxyl groups at the top of the serpentine layer below is not altered by rotation (about an axis

parallel to *z* passing through the middle of Si hexagons) of the top layer by any multiple of 60°. Rotation by 0°, 120°, or 240° gives completely identical layers because of the trigonal symmetry of each. Rotation by 60°, 180° or 300° gives identical layers as far as their tetrahedral components are concerned, but different configurations of the Mg ions and of the OH ions at the tops of layers. The effect of such a rotation on the *y* axis projection of the structure is illustrated in Fig. 4 and the two types of layer are referred to as *μ* and *γ* respectively. If every layer were rotated by *nπ/3* (where *n* is odd) with respect to its neighbour, a regular two-layered structure would result, corresponding approximately with that of ortho-chrysotile (Whittaker, 1956*b*). For reflexions with *l* = *m* + ½ only the Mg and OH ions contribute to the intensities so that these reflexions would be relatively weak, but for *l* = *m* the intensities are different from those for a single-layered structure, *i.e.* they correspond to a single-layered structure with half Mg and half OH in each of the alternative sites. It can be seen from Fig. 4 that for *h0l* reflexions with *h* = 6*m* the *μ* and *γ* layers are equivalent so that no *l* = *m* + ½ reflexions will occur.

A regular two-layered structure cannot, however, apply to the specimen considered here, since although

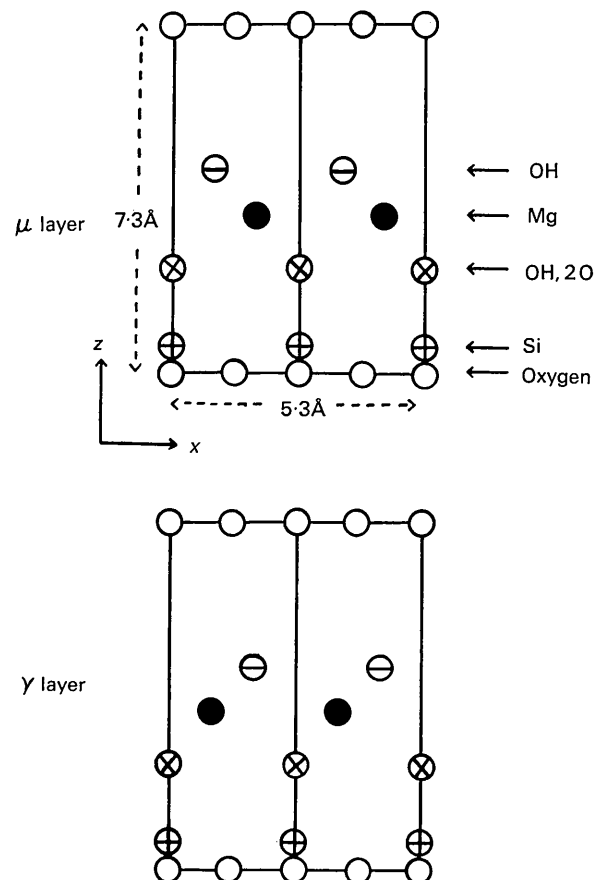


Fig. 4. *y*-axis projection of single layers of lizardite structure in *μ* and *γ* orientations.

intermediate  $h0l$  reflexions are observed except where  $h=6m$ , they are in this case diffuse not sharp, and moreover  $h0l$  and  $h0\bar{l}$  reflexions do not have equal intensities. The  $h0l$  and  $h0\bar{l}$  reflexions are for all crystals observed to be unequal, but are less different from one another than they would be for a regular one-layered structure.

An attempt was made to determine the diffraction effects which would be given in a crystal containing various mixtures of  $\mu$  and  $\gamma$  layers.

#### Model 1

The first model of this type considered has an equal number of  $\mu$  and  $\gamma$  layers and a probability  $\alpha$  that a stacking fault (*i.e.*  $\gamma$  follows  $\mu$  or  $\mu$  follows  $\gamma$ ) occurs. Using methods similar to those employed by Wilson (1962) it can be shown that the form of the intensity distribution is

$$I(w) = Q + \frac{P(1-s^2)}{1-2s \cos 2\pi w + s^2} \quad (1)$$

where  $w$  is the coordinate in reciprocal space parallel to  $c^*$ .

$Q$  is the part of the distribution which peaks at integral lattice points and is effectively zero elsewhere,

while the second term contains a generally diffuse continuous periodic function with peaks, the shape and positions of which are determined by  $\alpha$ .  $Q$  and  $P$  are given by:

$$Q = \left(\frac{A\mu + A\gamma}{2}\right)^2 + \left(\frac{B\mu + B\gamma}{2}\right)^2 \quad (3)$$

$$= \frac{1}{4}[F_\mu^2 + F_\gamma^2 + 2(A\mu A\gamma + B\mu B\gamma)] \quad (4)$$

$$P = \left(\frac{A\mu - A\gamma}{2}\right)^2 + \left(\frac{B\mu - B\gamma}{2}\right)^2 \quad (5)$$

$$= \frac{1}{4}[F_\mu^2 + F_\gamma^2 - 2(A\mu A\gamma + B\mu B\gamma)] \quad (6)$$

where  $A$  and  $B$  are respectively the real and imaginary parts of  $F$ . From equation (3) it can be seen that the main reflexions will be equal to those given by a single-layer cell with half atom occupancy of the two alternative sites. (These are also the intensities given by a regular two-layered  $\mu\gamma$  cell.) The intensity multiplied by the diffuse periodic function is determined by  $P$  which, as shown by equation (5), is very weak if the difference between  $\mu$  and  $\gamma$  layers is very small.

The form of the generally diffuse intensity distribution is illustrated in Fig. 5. For values of  $s$  between 1 (regular one layer) and 0 (random sequence) there is a peak centred on the reciprocal lattice point. This peak becomes flatter with decreasing  $s$ , while for values of  $s$  between 0 and  $-1$  (regular two-layer cell) the peak is centred at the midway position and becomes sharper as  $s$  approaches  $-1$ . For the model under consideration this sequence corresponds to a change in  $\alpha$  from 0 to  $\frac{1}{2}$ , and from  $\frac{1}{2}$  to 1.

Although the above model explains qualitatively the existence of diffuse regions midway between reciprocal lattice points, it is not compatible with the observed diffraction pattern, since for equal numbers of  $\mu$  and  $\gamma$  layers, no matter what the probability of a mistake,  $h0l$  and  $h0\bar{l}$  intensities would be equal, and they are observed to differ.

#### Model 2

Since the intensities of  $h0l$  and  $h0\bar{l}$  reflexions are in general not equal, there must be in the structure unequal numbers of  $\mu$  and  $\gamma$  layers. The treatment for model 1 was therefore extended to take account of a proportion  $f$  of  $\mu$  layers and  $g (= 1 - f)$  of  $\gamma$  layers. Also it is assumed that there is a probability  $\alpha$  that a  $\gamma$  layer

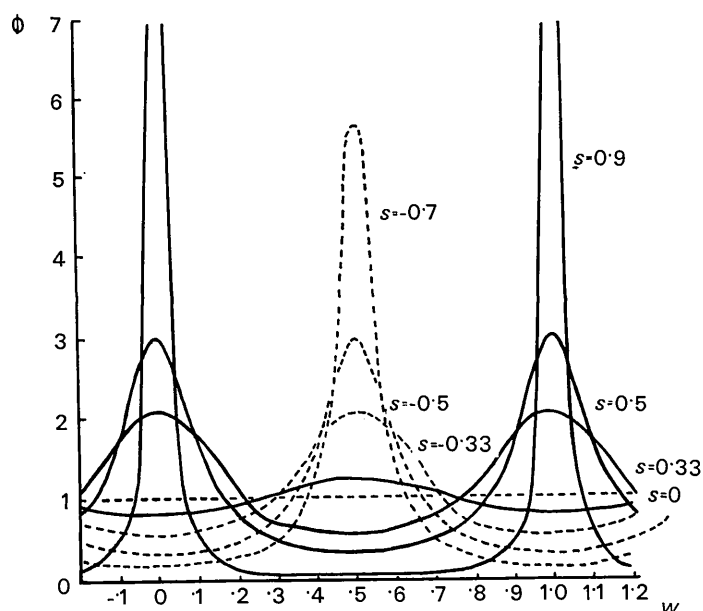


Fig. 5. A plot of the function:  $\phi = (1-s^2)/(1-2s \cos 2\pi w + s^2)$  for various values of  $s$ .

follows a  $\mu$  layer, and a probability  $\beta$  that a  $\mu$  follows a  $\gamma$  layer. It follows that

$$\alpha/\beta = g/f. \quad (7)$$

The form of the intensity distribution is again as given in equation (1) but now

$$Q = (fA\mu + gA\gamma)^2 + (fB\mu + gB\gamma)^2 \quad (8)$$

and

$$P = fg(A\mu - A\gamma)^2 + fg(B\mu - B\gamma)^2. \quad (9)$$

In the second term of equation (1), which gives the diffuse component of the intensity, the value of  $s$  now depends upon  $\alpha/g$  and it can be shown that

$$s = 1 - \alpha/g. \quad (10)$$

The integral breadth  $b$  of the diffuse component is given by

$$b = \frac{1 - 2s \cos 2\pi w + s^2}{1 - s^2}. \quad (11)$$

Thus for a peak at  $w=0$  or integer ( $s$  positive)

$$b = (1-s)/(1+s) \quad (12)$$

and for a peak at  $w = \text{integer} + \frac{1}{2}$  ( $s$  negative)

$$b = (1+s)/(1-s). \quad (13)$$

For the main reflexions, the intensities were calculated by equation (8) for different values of  $f$ , and the best agreement between  $F_o$  and  $F_c$  was obtained with  $f=0.7$ ; the measure of agreement obtained was  $R = \Sigma|F_o - F_c|/\Sigma|F_o| \simeq 21\%$ . This is an improvement over the value of  $R$  for the structure model with a regular one-layered cell. The values of  $F_c$  for  $f=0.7$  are listed in Table 3, column (a).

The profiles and positions of the diffuse peaks depend not only upon the distribution  $(1-s^2)/(1-2s \cos 2\pi w + s^2)$  but also on the way  $P$  varies with  $w$ , *i.e.* it is dependent also upon the  $A$  and  $B$  parts of the continuous transforms of the contents of  $\mu$  and  $\gamma$  cells. Thus the profiles of the various diffuse peaks are different, and only an approximate 'average integral breadth' measurement was made in the present case and was found to be  $b \simeq 0.35$ . Substituting this value in equations (13) and (10) gave  $\alpha/g = 1.5$ , so that with  $g=0.3$  ( $f=0.7$ ),  $\alpha \simeq 0.45$  and  $\beta \simeq 1.0$ .

On the basis of this model, therefore, the  $\mu$  and  $\gamma$  layers in lizardite are assumed to be present in the proportion 7:3 and are stacked in a partially disordered manner such that the probability that  $\gamma$  follows  $\mu$  is 0.45 and also so that a  $\mu$  layer is almost certain to follow a  $\gamma$ . This may also be taken to mean that the crystal is made up largely of  $\mu$  layers but that  $\gamma$  layers (approximately 30% of the total number, and mostly single) are interspersed.

The extent to which  $F_o$  values of  $h0l$  and  $h0\bar{l}$  reflexions differ is reasonably well matched in the  $F_c$  list, and it should be noted that the model described also has the merit of predicting the special relationships observed that, for reflexions with  $h$  and  $k$  both mul-

tiples of three, intensities  $hkl$  and  $hk\bar{l}$  are equal, and that no intermediate maxima occur along their particular Weissenberg festoons. For it can be shown that under these conditions

$$\begin{aligned} A\mu(hkl) &= A\mu(hk\bar{l}), & A\gamma(hkl) &= A\gamma(hk\bar{l}) \\ B\mu(hkl) &= -B\mu(hk\bar{l}), & B\gamma(hkl) &= -B\gamma(hk\bar{l}) \end{aligned}$$

and also that

$$A\mu(hkl) = A\gamma(hkl), \quad B\mu(hkl) = B\gamma(hkl)$$

so that from equation (8)

$$Q_{hkl} = Q_{hk\bar{l}}$$

and from equation (9)

$$P_{hkl} = 0.$$

This model satisfactorily explains the diffraction phenomena observed where the intermediate reflexions are diffuse, although it seems most unlikely from a theoretical point of view. It is difficult to understand why layers which differ only in orientation should be mixed in other than equal proportions. It was partly on account of this difficulty that more crystals were examined, to see if the intensity results and intermediate spot phenomena were general. As described earlier, some crystals were found which gave sharp intermediate spots while still maintaining  $h0l$  unequal to  $h0\bar{l}$  in the main series of reflexions. This result cannot be explained as a special case of model 2 since it can be shown that sharp reflexions at  $l=m+\frac{1}{2}$  can only be produced by equal numbers of  $\mu$  and  $\gamma$  layers, and that moreover, they would be accompanied by equal  $h0l$  and  $h0\bar{l}$  intensities.\*

### Model 3

Another possible model is a structure consisting of domains of wholly  $\mu$ , wholly  $\gamma$  or alternate  $\mu\gamma$  layers. This could be expressed quantitatively as having  $p\%$  of domains of  $\mu\mu$  two-layer cells, intermixed with  $q\%$  of  $\gamma\gamma$  two-layer cells, and  $r\%$  of  $\mu\gamma$  or  $\gamma\mu$  two-layer cells. Intensities contributed by each of the three types of domain were calculated and added in various proportions, and the agreement for the main reflexions ( $l=m$ ), as indicated by  $R$ , was plotted on a triangular diagram (Fig. 6). Best agreement was given by  $p=60$ ,  $q=10$ ,  $r=30\%$ , where  $R=18\%$  [Table 3, column (b)], an appreciable improvement over the earlier  $R=26\%$ . This model would thus explain satisfactorily the intensities of the main reflexions. The model does not explain why the intermediate reflexions, which arise solely from  $\mu\gamma$  domains, are generally diffuse, unless it is assumed also that there are mistakes in the  $\mu\gamma\mu\gamma\dots$  sequence.

\* If sharp reflexions are to occur from model 2 the integral breadth,  $b$ , of the spots must be small, tending to zero.

This condition is fulfilled as  $s \rightarrow -1$ .

If  $s = -1$ ,  $\alpha/g = \beta/f = 2$ .

Since  $g+f=1$ , then  $\alpha+\beta=2$ .

But neither  $\alpha$  nor  $\beta$  can be greater than 1; therefore  $\alpha = \beta = 1$ , and  $f = g = \frac{1}{2}$ .

These  $\mu\gamma$  domains with mistakes may then be considered by the same treatment as for model 1, where equal numbers of  $\mu$  and  $\gamma$  layers were proposed, but in this case we have equal numbers of  $\mu\gamma$  and  $\gamma\mu$  pairs. Let  $\alpha$  now be the probability that a mistake occurs after a  $\mu\gamma$  pair causing the next pair to be  $\gamma\mu$ . Variation in  $\alpha$  will affect the positions and sharpness of the non-integral reflexions. If  $\alpha$  is zero, sharp reflexions will occur at  $l=m+\frac{1}{2}$ , whereas if  $0 < \alpha < \frac{1}{2}$  these reflexions will be broad. Each of these circumstances is represented among the photographs obtained from the crystals studied.

If  $\frac{1}{2} < \alpha < 1$ , broad intermediate reflexions will occur at approximately  $l=m \pm \frac{1}{4}$  and none will be observed at  $l=m+\frac{1}{2}$ \*

The observation, for one crystal, of broad reflexions at  $l \approx m \pm \frac{1}{4}$  together with sharp reflexions at  $l=m+\frac{1}{2}$ , can be interpreted only if the two effects are produced by separate domains in the specimen and superimposed.

Model 3 is also satisfactory in explaining the special relationships for reflexions where both  $h$  and  $k$  are multiples of three.

For a normal single crystal the process of adding intensities from domains would be an artificial one, since with undistorted geometrical stacking successive layers would scatter with regular phase differences so that it would be necessary to combine  $F$ 's with appropriate phases rather than to add intensities. In the present case, however, the bending of the crystal may have the effect that a regular phase relationship will not be maintained over a large number of layers. Thus we may consider that there are independent though oriented crystallites with all  $\mu$ , all  $\gamma$ , or disordered  $\mu$  and  $\gamma$  layers scattering X-rays independently. The transition from a  $\mu$  to a  $\gamma$  block of layers can also be regarded as a form of twinning, and similarly the mistakes

in the disordered sequences as twinning on a very fine scale.

Model 3 satisfactorily explains the diffraction phenomena and though only calculated in detail for data from one crystal, it appears to be qualitatively applicable for all crystals from this particular specimen. Variations in the proportions of  $\mu$ ,  $\gamma$  and  $\mu\gamma$  domains, and in the probability of mistakes in the  $\mu\gamma$  regions are to be expected from crystal to crystal.

#### Broadened reflexions with $k \neq 3m$ or zero

The streaking of reflexions parallel to  $c^*$  when  $k \neq 3m$  or zero is similar to that described by Hendricks (1940) and indicates disorder of layer stacking with displacements of  $\pm b/3$ . It can be shown that the intensity distribution is given by

$$I_{(w)} = \frac{NF^2[1 - (1 - 3\alpha/2)^2]}{1 - 2(1 - 3\alpha/2)\cos 2\pi w + (1 - 3\alpha/2)^2} \quad (13)$$

[where  $\alpha$  is the probability of occurrence of a mistake in layer stacking and the integral breadth is given by  $b = 3\alpha/(4 - 3\alpha)$ ]. The profiles of 021 streaks measured on precession photographs gave a value of  $b \approx 0.5$  which corresponds to  $\alpha \approx \frac{2}{5}$ . This estimate of  $\alpha$  is necessarily very approximate since although the  $0kl$  streaks studied are not affected by the disorder of the layer rotations, they are affected by the crystal bending. It is of interest to note that the  $hkl$  reflexions with  $k \neq 3m$ , which were not studied in detail, will be affected by all three types of disorder, layer rotation, layer displacement, and crystal bending. The value of  $\alpha$  may also vary between crystals.

\* It can be shown from structural considerations that in this model the  $Q$  term of equation (1) is non-zero only at  $l=m$ .

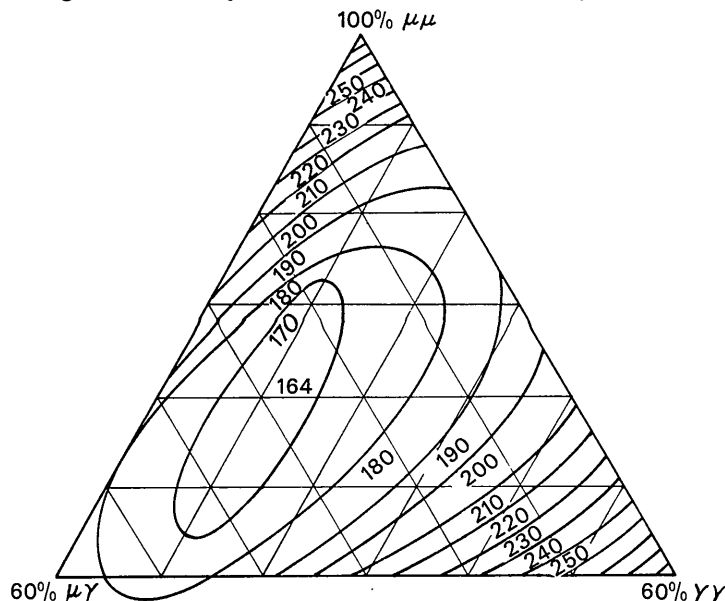


Fig. 6. Plot of  $\Sigma|F_0 - F_c|$  for the main reflexions  $20l$ ,  $40l$  and  $53l$ , assuming different proportions of  $\mu\mu \dots$ ,  $\gamma\gamma \dots$ , and  $\mu\gamma\mu\gamma \dots$  crystallites. Minimum at 60%  $\mu\mu$ , 10%  $\gamma\gamma$ , 30%  $\mu\gamma$ .

**Summary**

For the lizardite variety of serpentine from Kennack Cove, Cornwall, X-ray diffraction single-crystal methods confirm the basic serpentine structure and show that the crystals are disordered in three different ways. (1) Non-Bragg diffraction maxima and the intensities of other reflexions show that individual serpentine layers may be rotated by  $\pm 60^\circ$  or  $180^\circ$ ; these layers are most probably stacked in domains some of which are in one-layer sequences in either orientation, and others in alternating sequences with a two-layer repeat. The latter exhibit sequences containing mistakes, the probability of which varies from one crystal to another, and possibly also from one domain to another within a single crystal. (2) Reflexions with  $k \neq 3m$ , which are streaked parallel to  $c^*$ , show that layers may be displaced by  $\pm b/3$ , and the probability of a stacking mistake is approximately 0.4. (3) Reflexions are spread along powder arcs indicating considerable curvature of the crystal on a macroscopic scale, so that its habit approximates to a spherical cap.

The 'average' structure (*i.e.* layer shifts and rotations averaged over the whole crystal) has trigonal symmetry, but the ortho-hexagonal cell with  $b = a\sqrt{3}$  is used for its description.

In view of the above results, it may be conjectured that different lizardite specimens may exhibit translational and rotational disorder to varying degrees, and also that multi-layered regular sequences additional to those already described for serpentine structures

(*e.g.* 6-layered, Zussman & Brindley, 1957; Gillery, 1959; Lapham 1961) may occur. The Kennack specimen is exceptional in that other lizardites are too fine-grained for single-crystal X-ray work. In powder patterns of the fine lizardites, non-Bragg maxima and other diffuse reflexions may be too weak to be observed, but the relative intensities of the main reflexions might be expected to show some variations. Such effects, however, would be reduced in powder patterns because of the coincidence of  $hkl$  and  $\bar{h}\bar{k}l$  reflexions owing to the dimensional symmetry of the crystal lattice.

One of us (J.C.R.) wishes to express his appreciation to the Education Committee of the City of Carlisle for financial support during part of this work.

**References**

- GILLERY, G. H. (1959). *Amer. Min.* **44**, 143.  
 HENDRICKS, S. B. (1940). *Phys. Rev.* **57**, 448.  
 KUNZE, G. (1956). *Z. Kristallogr.* **108**, 82.  
 KUNZE, G. (1958). *Z. Kristallogr.* **110**, 282.  
 KUNZE, G. (1961). *Fortschr. Min.* **39**, 206.  
 LAPHAM, D. M. (1961). *Amer. Min.* **46**, 168.  
 MIDGLEY, H. G. (1951). *Miner. Mag.* **29**, 526.  
 WHITTAKER, E. J. W. (1956a). *Acta Cryst.* **9**, 855.  
 WHITTAKER, E. J. W. (1956b). *Acta Cryst.* **9**, 862.  
 WHITTAKER, E. J. W. & ZUSSMAN, J. (1956). *Miner. Mag.* **31**, 107.  
 WILSON, A. J. C. (1962). *X-ray Optics*. London: Methuen.  
 ZUSSMAN, J. & BRINDLEY, G. W. (1957). *Amer. Min.* **42**, 666.

*Acta Cryst.* (1965). **19**, 389

## The Crystal Structure of Bisnitratodiaquodioxouranium(VI) Tetrahydrate (Uranyl Nitrate Hexahydrate)

BY D. HALL, A. D. RAE AND T. N. WATERS

*Chemistry Department, University of Auckland, New Zealand*

(Received 7 December 1964)

The crystal structure of uranyl nitrate hexahydrate has been refined in three dimensions. The uranium atom is 8-coordinate, with the two nitrate ions (as bidentate ligands) and the two water molecules coordinated in the plane perpendicular to the uranyl group. The molecule is involved with the water of crystallization in an extensive hydrogen-bonding system, which apparently causes some distortion from the ideal molecular shape.

The structure determination of the hexahydrate of uranyl nitrate by Fleming & Lynton (1960) has shown the compound to be correctly formulated  $[\text{UO}_2(\text{NO}_3)_2(\text{H}_2\text{O})_2]4\text{H}_2\text{O}$ , with the nitrate ions acting as bidentate chelating groups. The structure was studied in projection, and only in one such projection was satisfactory refinement possible. The reported parameters are then at best of low precision, and many apparently interesting features of the molecule, *e.g.* the non-linear uranyl ion, must be treated with some reserve. We have

redetermined this structure, and have refined the parameters using three-dimensional procedures.

**Experimental**

Suitable crystals were available from a commercial sample without recrystallization. The dimensions of the orthorhombic unit cell were obtained from Weissenberg photographs by the method of Main & Woolfson (1963) as  $a = 13.18 \pm 0.01$ ,  $b = 8.00 \pm 0.02$ ,  $c = 11.47 \pm$